RSC Advances

COMMUNICATION

View Article Online
View Journal | View Issue

Cite this: *RSC Adv.*, 2016, **6**, 36834

Received 22nd March 2016
Accepted 5th April 2016

DOI: 10.1039/c6ra07518e

www.rsc.org/advances

Adsorption of pure SO_2 on nanoscaled graphene oxide†

Deepu J. Babu,‡[a] Frank G. Kühl,‡[b] Sandeep Yadav,[a] Daniel Markert,[a] Michael Bruns,[c] Manfred J. Hampe[b] and Jörg J. Schneider*[a]

Adsorption of pure SO_2 is studied for the first time on graphene oxide (GO). The adsorption mechanism was found to be fundamentally different from conventional carbon materials like activated carbon or carbon fibers. It was observed that GO binds SO_2 only by physisorption ($\Delta H_{ads} = 18.04$ kJ mol^{-1}) and still the adsorption capacity was found to be comparable to traditional adsorbents like activated carbon or carbon molecular sieves. The 2D layered morphology as well as the absence of extensive micropores well known to promote SO_2 to SO_3 conversion are responsible for the observed physisorption characteristics.

Sulfur compounds, especially sulfur dioxide SO_2 and sulfur trioxide SO_3, are found as hazardous compounds in industrial burning processes of fossil fuels *e.g.* coal, natural gas, oil. Even at low concentrations they are corrosive and toxic, thus presenting an immense threat to the environment. In contact with water vapor from the atmosphere they react to form sulfonic and sulfuric acid, which are the main reasons for acid rain causing extensive environmental damage. SO_2 removal techniques can be categorized into two broad classes namely absorption in liquids and sorption by solids.[1,2] Conventional absorption process like limestone scrubbing or ammonia scrubbing have some inherent disadvantages like secondary pollution, large water and energy consumption *etc.*[1,3] Adsorptive removal of SO_2 is a promising technique due to simplicity of operation and maintenance as well as the possibility to regenerate and fully reuse the spent adsorbent. An ideal adsorbent should have a high adsorption capacity at near ambient conditions, should be stable under process conditions and easily regenerable. Though zeolites and metal organic framework compounds (MOF) have a high adsorption capacity arising from their predominantly microporous framework, the presence of moisture in combination with the corrosive nature of SO_2 and SO_3 are detrimental to the long term stability of these adsorbents.[4] Due to its better stability under such conditions, carbon based materials especially activated carbon and carbon fibers are the most widely used adsorbents for SO_2 recovery.[5–9] SO_2 is however known to adsorb on carbon materials both physically as well as chemically.[10,11] A complete desorption is typically not observed for activated carbon materials exposed to SO_2 even under dry conditions and low concentrations. The presence of micropores (close to 0.7 nm), humidity and oxygen in the gaseous phase is known to further facilitate chemisorption of SO_2.[12,13] Though chemisorption promotes higher adsorption, regeneration of the adsorbent not only becomes energy intensive but also involves the consumption of the adsorbent and simultaneous generation of CO_2.[1]

Recently, graphene oxide (GO) has attracted a great deal of interest in the field of energy and gas storage as well as catalysis.[14–17] This is driven by the tunability of the material in terms of its surface area, porosity and extent of oxygen surface functionalization and last but not least to its straightforward accessibility. Its mechanically stable sp^2 carbon framework, the presence of considerable amount of oxygen functionalities distributed along the interlayers and the possibility of large-scale synthesis from inexpensive starting material qualifies GO as a plausible adsorbent material for SO_2 adsorption. So far, only very few studies have investigated the SO_2 adsorption characteristics of GO. Most of these studies are either purely theoretical or experimental works dealing with ppm concentrations of SO_2 gas adsorption.[18–21] However, equilibrium adsorption data of pure SO_2 gas is of great significance for theoretical studies on the subject as well as for predicting gas selectivity, when it comes to studying selective adsorption of gas mixtures. To the best of our knowledge no experimental

[a]*Eduard-Zintl-Institut für Anorganische und Physikalische Chemie, Technische Universität Darmstadt, Alarich-Weiss-Strasse 12, 64287 Darmstadt, Germany. E-mail: joerg.schneider@ac.chemie.tu-darmstadt.de*

[b]*Fachgebiet Thermische Verfahrenstechnik, Technische Universität Darmstadt, Otto-Berndt-Straße 2, 64287 Darmstadt, Germany*

[c]*Institute for Applied Materials (IAM-ESS) and Karlsruhe Nano Micro Facility (KNMF), Karlsruhe Institute of Technology (KIT), Hermann-von-Helmholtz-Platz 1, 76344 Eggenstein-Leopoldshafen, Germany*

† Electronic supplementary information (ESI) available. See DOI: 10.1039/c6ra07518e

‡ Both authors contributed equally to this work.

adsorption data on GO in pure SO_2 atmosphere at ambient or elevated pressures are available in the literature so far.

Herein we investigate the fundamental adsorption characteristics of GO towards pure SO_2. To this end, pure SO_2 atmosphere rather than a flue gas composition is chosen, as it is known that the presence of oxygen and moisture influences SO_2 adsorption on carbon materials. Moreover, the nature of gas adsorption and hysteresis effects upon loading and deloading becomes more evident under pure gas atmosphere when both processes are unaffected by any further reaction chemistry *e.g.* with water. Furthermore CO_2 adsorption on GO is carried out to understand the influence of the dipole moment of both gases on the observed adsorption characteristics [$\mu(SO_2) = 1.6$ D, $\mu(CO_2) = 0$]. The effect of selective nitrogen functionalization on the surface of GO towards SO_2 and CO_2 adsorption is investigated as well.

For the preparation of graphene oxide (GO) (Fig. 1) graphite was first oxidized to graphite oxide according to the improved synthesis technique of Marcano *et al.* [ref. 22 and ESI† for details]. A combination of ultrasound sonication followed by various freeze–thaw cycles[23] was successfully employed to exfoliate graphite oxide to produce GO (see ESI† for more details). CO_2 adsorption measurement on this material was carried out in a modified thermogravimetric (TG) setup and high pressure SO_2 adsorption measurements were carried out in a commercial gravimetric setup (Rubotherm, Bochum, see ESI† for details).

N_2 adsorption isotherms were measured to determine the porosity and specific surface area before and after exfoliation. A negligible amount of nitrogen is adsorbed in the as-prepared graphite oxide (see Fig. S1 in ESI†) and consequently graphite oxide exhibits a very low specific surface area of 6 m^2 g^{-1}. Significant improvement in surface area is observed upon exfoliation. N_2 adsorption isotherm of GO is shown in Fig. 2a. GO exhibits a type-IV isotherm in accord with previous reports[17] and has a BET surface area of 268 m^2 g^{-1}. Unlike activated carbons, which typically exhibits a type-I adsorption isotherm, no steep increase in adsorption is found at low pressures indicating the absence of extensive micropores. An SEM image of the GO is shown in the inset of Fig. 2a. The 2D layered morphology can be inferred from SEM and the characteristic wrinkled, layer like morphology of GO[24] becomes evident from TEM (Fig. 2b).

Fig. 1 Schematic of the synthesis process of GO (synthesis and exfoliation) starting from commercial graphite.

Raman spectra of as-prepared graphite oxide and GO are given in Fig. 3a. The two prominent peaks are the graphitic peak (G-band) at ~1585 cm^{-1} and the defect induced peak (D-band) at 1350 cm^{-1}. The G-band gives the Raman signature for all sp^2 carbon materials and the D-band is activated only in the presence of defects.[25] The higher D-band observed in both cases is typical for graphite/graphene oxide materials and is an indicator of the structural distortions induced by the attachment of a large number of functional groups.[26] The I_D/I_G ratio of graphite oxide is determined to be 0.96 and after exfoliation, the ratio decreased slightly to 0.91. The small improvement in I_D/I_G ratio observed might be due to the removal of some functional groups during the exfoliation procedure. It is known that exfoliation leads to the breakage of hydrogen bonds between adsorbed water and surface functional groups.[14] Nevertheless, significant amounts of functional groups still remain on the surface. X-ray photoelectron (XPS) survey spectrum of GO indeed confirms the presence of oxygen on the surface (see Fig. S2 and Table 1 in ESI†). To determine the nature and type of C–O bonding, the C 1s spectrum obtained under high resolution is deconvoluted into 3 peaks as shown in Fig. 3b. The main peak at 284.4 eV corresponds to the sp^2 bonded carbon and the other peaks are assigned to C–O (286.1 eV) and O–C=O (288.3 eV). The parameters for the asymmetric peak shape of the component at 284.4 eV are based on the peak shape originating from high purity CNT.[27]

CO_2 adsorption measurements were carried out on GO at 1 bar and 35 °C. Prior to the measurement, the sample was heated to 300 °C in an argon atmosphere (see also ESI†). The exfoliated samples adsorbed ~24.9 mg g^{-1} of CO_2 at 35 °C as shown in Fig. 4a. Since the measurements are carried out on a modified TG setup, a continuous monitoring of the sample mass is possible. A significant weight loss of ~7.05% is observed already during the preliminary heating to 300 °C. In agreement with the reported TG and XPS studies,[16,26] the observed weight loss may be attributed to the loss of oxygen functional groups.

To investigate the effect of these weight loss on the CO_2 adsorption characteristics, adsorption measurements were carried out on a sample which was heated only to 150 °C. In this case, only 2.3% decrease in weight loss was observed. However, the adsorption capacity of this sample decreased slightly to 22.4 mg g^{-1} (Fig. 4a) as the sample activation temperature is lowered from 300 °C to 150 °C. Heat treatment of GO is known to remove surface functional groups leading to the creation of pores on the GO structure.[28] Increase in adsorption capacity with an increase in activation temperature is therefore in agreement with the higher porosity of the sample heated at 300 °C.

Previous studies on activated carbon[29] and GO[30] have shown that the extent of nitrogen functionalization on these materials

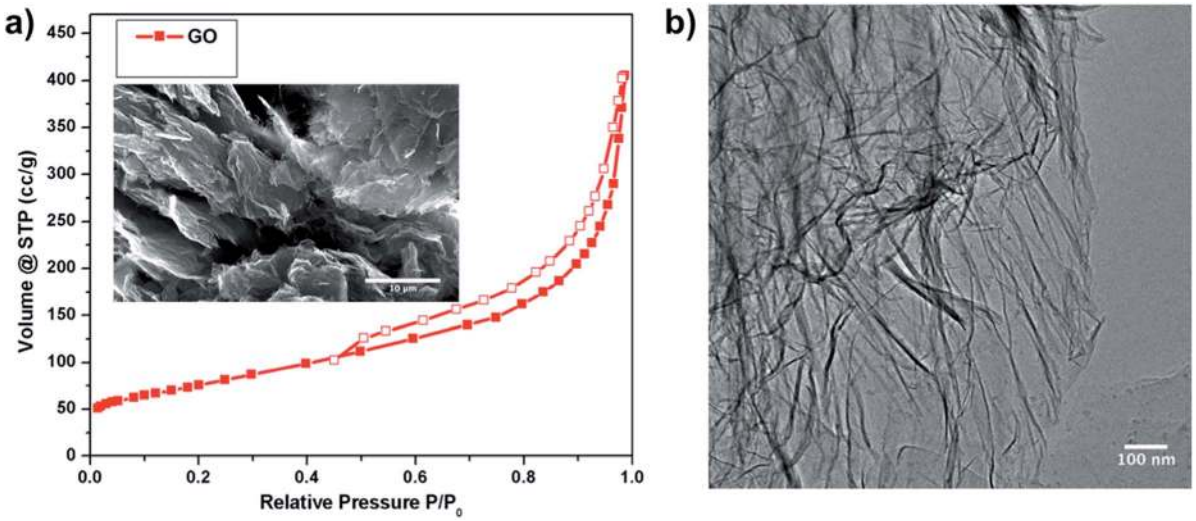

Fig. 2 (a) N_2 adsorption isotherm of GO, closed symbols represents the adsorption trace, open symbols represents desorption trace. Inset in (a) shows the SEM image (scale bar = 10 μm) of GO, (b) TEM image (scale bar = 100 nm) of GO.

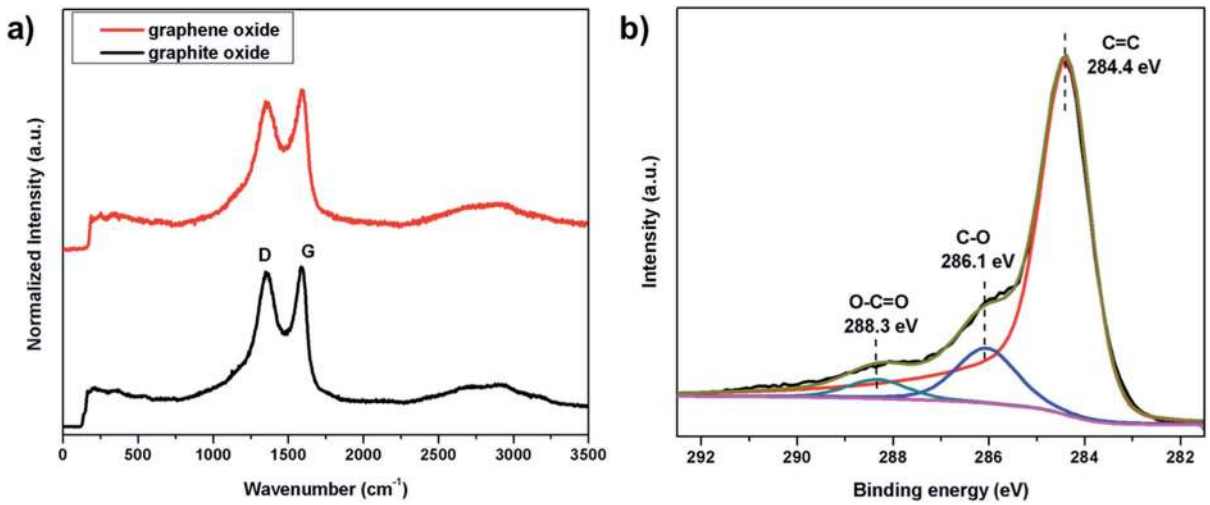

Fig. 3 (a) Raman spectra of as-prepared graphite oxide and graphene oxide (GO). (b) Experimental high resolution C 1s XPS spectrum of GO together with signal fitting.

depend on their initial oxygen surface functionalization. GO inherently has a range of various oxygen functional groups and is therefore ideally suited to introduce a significant amount of nitrogen containing surface groups by chemical modification (conversion) of initial oxygen functionalities. To determine the effect of nitrogen containing functional groups on the surface of GO on CO_2 and SO_2 gas adsorption, GO was treated with a N_2 rf plasma for 60 minutes which introduces a significant amount of nitrogen containing functionalities (see ESI† for more details). No morphological changes were observed in SEM upon this treatment (Fig. S3 in ESI†). N_2 adsorption isotherms (Fig. S4 in ESI†) of N_2 plasma treated GO were almost identical to that of GO (Fig. S4 in ESI†). In addition, plasma treatment did not significantly alter the specific surface of GO and was determined to be ~264 $m^2\ g^{-1}$. This value is only slightly lower than in the as prepared GO material. Raman measurements of the nitrogen functionalized GO showed an increase in D-band intensity and I_D/I_G ratio increased from 0.91 to 0.97 after 60 minutes of N_2 plasma treatment (see Fig. S5 in ESI†).

High energy electrons and ions in an rf plasma are known to induce structural defects in the graphene lattice explaining this observed increase.[31,32] The XPS survey spectrum confirms the successful generation of nitrogen functionalities on GO (~3.5%) by rf plasma treatment (see Fig. S6 in ESI†). Deconvolution of the high resolution C 1s spectrum (Fig. S6b in ESI†), revealed the additional presence of a new peak at 287.1 eV attributed to C=N–C groups.[33] Moreover, the shift of the C–O component to lower binding energies (Fig. S6c in ESI†) indicates the formation of additional C–NH. To determine the nature of the nitrogen functionalities, the high-resolution N 1s

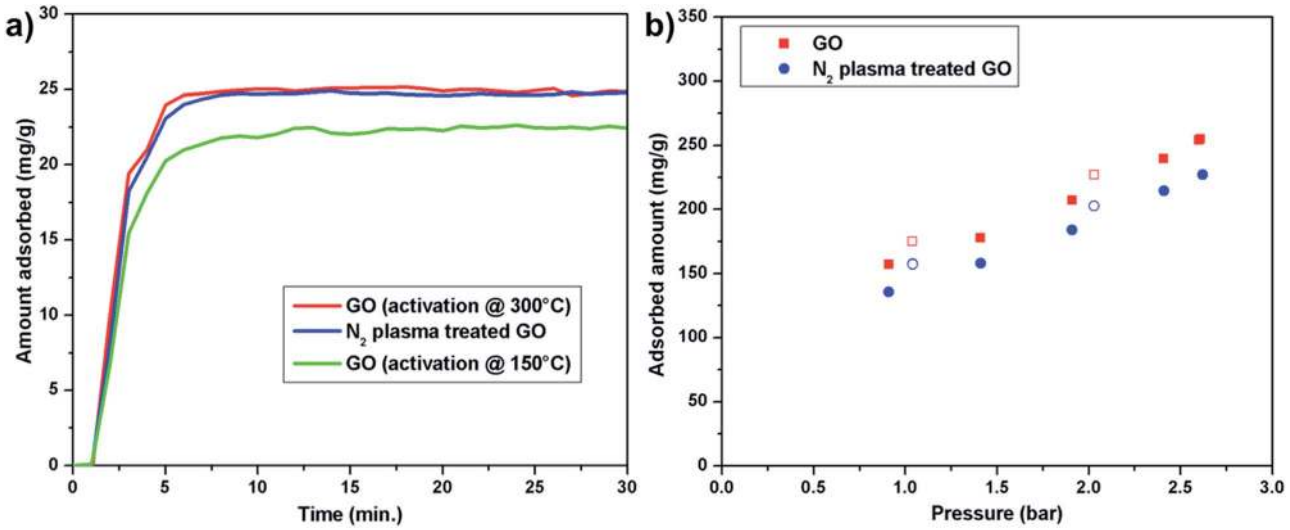

Fig. 4 (a) CO_2 adsorption at 35 °C and 1 bar (b) SO_2 adsorption at 25 °C, the closed symbols represent adsorption and the open symbol represents desorption.

spectrum is deconvoluted (Fig. S6d in ESI†) and the signals fitted corresponding (i) to C=N–C (398.7 eV) and (ii) C–NH (400.0 eV) nitrogen functionalities.[34]

CO_2 adsorption studies on such a N_2 plasma treated sample activated at 300 °C, however showed no improvement in adsorption characteristics at 1 bar and 35 °C compared to GO as shown in Fig. 4a. Tamilarasan *et al.*[35] have reported an enhanced CO_2 adsorption for N_2 plasma treated hydrogen exfoliated GO. They have observed an increase of ~2 mg g^{-1} for N_2 plasma treated sample over untreated GO, however at 10 °C. In the present case, the relevant measurement is carried out at 35 °C. As gas adsorption (physisorption) typically diminishes at higher temperatures, this explains the observed difference of CO_2 adsorption in both experiments.

Pure SO_2 adsorption isotherm measurements were carried out on GO at 25 °C up to the supply pressure which is close to the saturation pressure of the adsorbate gas. The amount of pure SO_2 adsorbed on GO is much higher when compared to pure CO_2 adsorption under similar conditions of temperature and pressure (see Fig. 4b). This is attributed to the stronger van der Waals interaction resulting from the larger dipole moment of SO_2 compared to CO_2 under these adsorption conditions. Near ambient pressure, GO has an SO_2 adsorption capacity of 156 mg g^{-1}. With an increase in pressure the adsorption capacity increases to 257 mg g^{-1} at 2.6 bar. GO with its moderate specific surface area of 268 m^2 g^{-1} exhibits an adsorption capacity at par with other carbon materials like activated carbon, carbon molecular sieves or activated carbon fibers[36,37] which typically have very large specific surface areas. For example Bae *et al.*[36] observed an adsorption capacity of close to 3 mmol g^{-1} for carbon molecular sieves at around 2.6 bar while at the same pressure, GO exhibits an adsorption capacity of more than 4 mmol g^{-1}.

Desorption measurements indicated an almost complete unloading of the adsorbed SO_2 with barely no hysteresis under ambient conditions. It is known from detailed studies on activated carbons and carbon fibers that SO_2 adsorbs on carbon materials resulting in the presence of two different adsorption regimes.[10,11] Weakly adsorbed SO_2 is the main adsorbate in regime one (adsorption energy $\leq$ 50 kJ mol^{-1}) and strongly adsorbed SO_2 constitutes adsorption regime two (adsorption energy > 80 kJ mol^{-1}). In the latter, oxidation of SO_2 to SO_3 occurs which results in a subsequently stronger adsorption by chemisorption compared to SO_2 which is only physisorbed in regime one. Consequently, desorption of the more strongly adsorbing SO_3 requires significant higher temperatures up to 300 °C compared to that for SO_2. We have carried out desorption of SO_2 by releasing the pressure which allows for an almost complete desorption of SO_2 adsorbed which is purely physisorbed on the GO surface. The 2D layered morphology as well as the absence of extensive micropores (which is known to promote SO_2 to SO_3 conversion[12]) is expected to be main reason for the observed physisorption characteristics.

To further confirm the predominant physisorption process of pure SO_2 on GO, adsorption isotherms were measured at 288 K and 308 K. As seen from Fig. 5a, the adsorption capacity decreased with an increase in temperature indicating again a physisorption mechanism. Isosteric heat of adsorption was calculated by fitting the isotherms using a virial type equation.[38] The heat of adsorption thus calculated is found to be 18.04 kJ mol^{-1} at 0.5 mmol g^{-1} loading and decreases with an increase in loading as shown in Fig. 5b (see ESI† for details). This significantly low heat of adsorption manifests clearly the physisorption nature of SO_2 adsorption on GO.

SO_2 adsorption measurements were also performed on N_2 plasma functionalized GO at 25 °C as shown in Fig. 4b. Contrary to the reports on activated carbon and activated carbon fibers,[39–42] no enhancement in adsorption capacity is observed after the introduction of various nitrogen functionalities. This again points to the different mechanism of SO_2 adsorption on GO compared to other activated carbon materials.

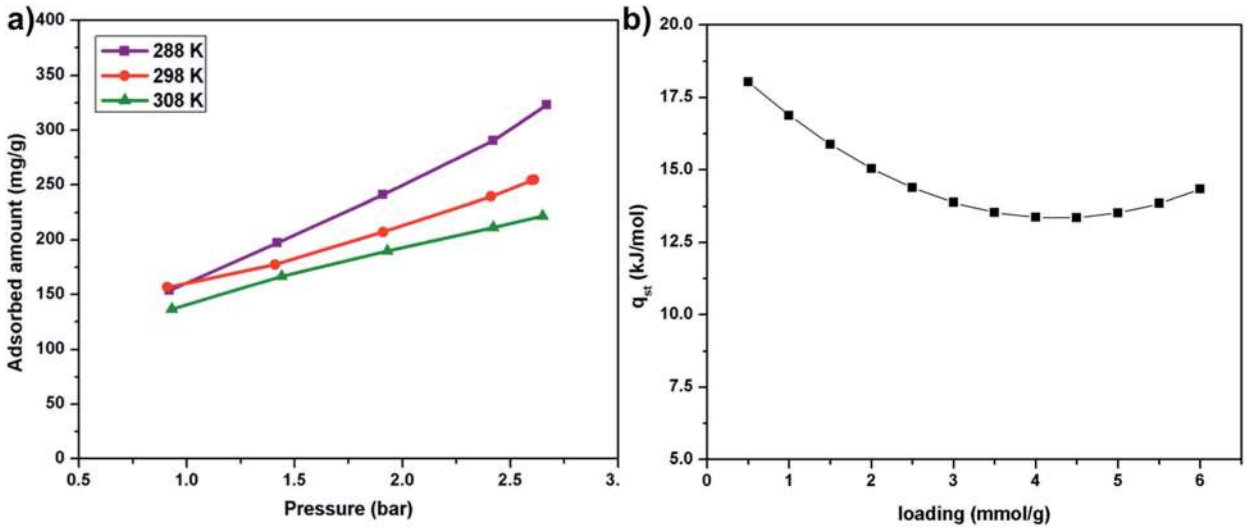

Fig. 5 (a) SO_2 adsorption on GO at 288, 298 and 308 K. (b) Isosteric heat of adsorption as a function of loading.

Conclusion

CO_2 and SO_2 adsorption measurements were carried out on exfoliated graphene oxide (GO) samples. The adsorption capacity of GO is found to vary with the activation temperature. Under similar conditions of temperature and pressure, GO exhibited a greater affinity for pure SO_2 over pure CO_2. Even with a significant amount of oxygen functionalities on the surface of GO, no chemisorption of SO_2 was observed. Pure SO_2 is found to physisorb with a low isosteric heat of adsorption of 18.04 kJ mol^{-1} on GO and the adsorption capacity is found to be still comparable to that of other porous carbon materials. Therefore GO qualifies for swing adsorption studies of SO_2. N_2 plasma treatment leads to ~3.5 at% nitrogen functionalization on the GO surface however, no noticeable improvement in CO_2 or SO_2 adsorption is observed with this material over native GO. The 2D layered morphology and the absence of the extensive micropores is supposed to be the reason for the observed difference from other traditional carbon materials.

Acknowledgements

The authors acknowledge MSc. Sherif Okeil for Raman and Dr Jörg Engstler for TEM measurements (TEM was done under contract ERC-TUD1 at ERC Jülich, Germany). XPS measurements were carried out under the KNMF program at KIT, Karlsruhe, Germany (proposal 2015-014008109). DJB and JJS acknowledge the DFG priority program 1570 for continuous financial support.

Notes and references

1 D. Stirling, *The Sulfur Problem*, Royal Society of Chemistry, Cambridge, 2000.
2 B. G. Miller, *Fossil Fuel Emissions Control Technologies: Stationary Heat and Power Systems*, Elsevier Science, 2015.
3 I. Mochida, Y. Korai, M. Shirahama, S. Kawano, T. Hada, Y. Seo, M. Yoshikawa and A. Yasutake, *Carbon*, 2000, **38**, 227–239.
4 J. Liu, A. I. Benin, A. M. B. Furtado, P. Jakubczak, R. R. Willis and M. D. LeVan, *Langmuir*, 2011, **27**, 11451–11456.
5 A. L. Kohl and R. Nielsen, *Gas Purification*, Gulf Professional Publishing, 1997.
6 S. Kisamori, I. Mochida and H. Fujitsu, *Langmuir*, 1994, **10**, 1241–1245.
7 J. A. DeBarr, A. A. Lizzio and M. A. Daley, *Energy Fuels*, 1997, **11**, 267–271.
8 A. Lisovskii, G. E. Shter, R. Semiat and C. Aharoni, *Carbon*, 1997, **35**, 1645–1648.
9 P. Davini, *Carbon*, 2003, **41**, 277–284.
10 P. Davini, *Carbon*, 1990, **28**, 565–571.
11 C. Moreno-Castilla, F. Carrasco-Marfn, E. Utrera-Hidalgo and J. Rivera-Utrilla, *Langmuir*, 1993, **9**, 1378–1383.
12 E. Raymundo-Piñero, D. Cazorla-Amorós, C. Salinas-Martinez de Lecea and A. Linares-Solano, *Carbon*, 2000, **38**, 335–344.
13 A. A. Lizzio and J. A. DeBarr, *Energy Fuels*, 1997, **11**, 284–291.
14 D. R. Dreyer, S. Park, C. W. Bielawski and R. S. Ruoff, *Chem. Soc. Rev.*, 2010, **39**, 228–240.
15 Y. Long, C. Zhang, X. Wang, J. Gao, W. Wang and Y. Liu, *J. Mater. Chem.*, 2011, **21**, 13934.
16 G. Srinivas, J. W. Burress, J. Ford and T. Yildirim, *J. Mater. Chem.*, 2011, **21**, 11323.
17 G. Srinivas, J. Burress and T. Yildirim, *Energy Environ. Sci.*, 2012, **5**, 6453.
18 H. Zhang, W. Cen, J. Liu, J. Guo, H. Yin and P. Ning, *Appl. Surf. Sci.*, 2015, **324**, 61–67.
19 M. Seredych and T. J. Bandosz, *J. Phys. Chem. C*, 2010, **114**, 14552–14560.
20 L. Shao, G. Chen, H. Ye, Y. Wu, Z. Qiao, Y. Zhu and H. Niu, *Eur. Phys. J. B*, 2013, **86**, 54.

21 C. Chen, K. Xu, X. Ji, L. Miao and J. Jiang, *Phys. Chem. Chem. Phys.*, 2014, **16**, 11031–11036.
22 D. C. Marcano, D. V Kosynkin, J. M. Berlin, A. Sinitskii, Z. Sun, A. Slesarev, L. B. Alemany, W. Lu and J. M. Tour, *ACS Nano*, 2010, **4**, 4806–4814.
23 I. Ogino, Y. Yokoyama, S. Iwamura and S. R. Mukai, *Chem. Mater.*, 2014, **26**, 3334–3339.
24 Y. Shao, J. Wang, M. Engelhard, C. Wang and Y. Lin, *J. Mater. Chem.*, 2010, **20**, 743–748.
25 A. Jorio, M. S. Dresselhaus, R. Saito and G. Dresselhaus, *Raman Spectroscopy in Graphene Related Systems*, John Wiley & Sons, 2011.
26 D. Yang, A. Velamakanni, G. Bozoklu, S. Park, M. Stoller, R. D. Piner, S. Stankovich, I. Jung, D. A. Field, C. A. Ventrice and R. S. Ruoff, *Carbon*, 2009, **47**, 145–152.
27 N. Zydziak, C. Hübner, M. Bruns, A. P. Vogt and C. Barner-Kowollik, *Polym. Chem.*, 2013, **4**, 1525–1537.
28 L.-Y. Meng and S.-J. Park, *J. Colloid Interface Sci.*, 2012, **386**, 285–290.
29 C. Pevida, M. G. G. Plaza, B. Arias, J. Fermoso, F. Rubiera and J. J. J. Pis, *Appl. Surf. Sci.*, 2008, **254**, 7165–7172.
30 X. Li, H. Wang, J. T. Robinson, H. Sanchez, G. Diankov and H. Dai, *J. Am. Chem. Soc.*, 2009, **131**, 15939–15944.
31 D. J. Babu, M. Lange, G. Cherkashinin, A. Issanin, R. Staudt and J. J. Schneider, *Carbon*, 2013, **61**, 616–623.
32 D. J. Babu, S. Yadav, T. Heinlein, G. Cherkashinin and J. J. Schneider, *J. Phys. Chem. C*, 2014, **118**, 12028–12034.
33 E. H. Lock, D. Y. Petrovykh, P. Mack, T. Carney, R. G. White, S. G. Walton and R. F. Fernsler, *Langmuir*, 2010, **26**, 8857–8868.
34 S. Engin, V. Trouillet, C. M. Franz, A. Welle, M. Bruns and D. Wedlich, *Langmuir*, 2010, **26**, 6097–6101.
35 P. Tamilarasan and S. Ramaprabhu, *J. Appl. Phys.*, 2015, **117**, 144301.
36 Y.-S. Bae and C.-H. Lee, *Carbon*, 2005, **43**, 95–107.
37 H. Yi, Z. Wang, H. Liu, X. Tang, D. Ma, S. Zhao, B. Zhang, F. Gao and Y. Zuo, *J. Chem. Eng. Data*, 2014, **59**, 1556–1563.
38 L. Czepirski and J. JagieŁŁo, *Chem. Eng. Sci.*, 1989, **44**, 797–801.
39 A. Bagreev, S. Bashkova and T. J. Bandosz, *Langmuir*, 2002, **18**, 1257–1264.
40 E. Raymundo-Piñero, D. Cazorla-Amorós and A. Linares-Solano, *Carbon*, 2003, **41**, 1925–1932.
41 C. L. Mangun, J. A. DeBarr and J. Economy, *Carbon*, 2001, **39**, 1689–1696.
42 K. Li, L. Ling, C. Lu, W. Qiao, Z. Liu, L. Liu and I. Mochida, *Carbon*, 2001, **39**, 1803–1808.